

Article

Not peer-reviewed version

Annealing of Oxygen-Related Frenkel Defects in Corundum Single Crystals Irradiated with Energetic Xenon Ions

[Eugene Kotomin](#)^{*}, [Ruslan Assylbaev](#), [Guldar Baubekova](#), Irina Kudryavtseva, [Vladimir N Kuzovkov](#), [Alise Podelinska](#), [Viktor Seeman](#), [Jevgeni Shablonin](#), [Aleksandr Lushchik](#)

Posted Date: 26 May 2025

doi: 10.20944/preprints202505.1919.v1

Keywords: Al₂O₃; Radiation; Swift heavy ions; Radiation-induced absorption; Frenkel defects; Diffusion-controlled annealing



Preprints.org is a free multidisciplinary platform providing preprint service that is dedicated to making early versions of research outputs permanently available and citable. Preprints posted at Preprints.org appear in Web of Science, Crossref, Google Scholar, Scilit, Europe PMC.

Copyright: This open access article is published under a Creative Commons CC BY 4.0 license, which permit the free download, distribution, and reuse, provided that the author and preprint are cited in any reuse.

Article

Annealing of Oxygen-Related Frenkel Defects in Corundum Single Crystals Irradiated with Energetic Xenon Ions

E.A. Kotomin ^{1,*}, R. Assylbayev ², G. Baubekova ³, I. Kudryavtseva ⁴, V.N. Kuzovkov ¹, A. Podelinska ⁴, V. Seeman ⁴, E. Shablonin ⁴ and A. Lushchik ⁴

¹ Institute of Solid State Physics, University of Latvia, Kengaraga 8, Riga LV-1063, Latvia

² Margulan University, Toraigyrov str. 58, 140000 Pavlodar, Kazakhstan

³ L.N. Gumilyov Eurasian National University, Munaitpasov Str. 13, 010008 Astana, Kazakhstan

⁴ Institute of Physics, University of Tartu, W. Ostwald Str. 1, 50411 Tartu, Estonia

* Correspondence: kotomin@latnet.lv

Abstract: The recovery of radiation damage induced by 231-MeV xenon ions with varying fluence (from 5×10^{11} and 2×10^{14} cm⁻²) in α -Al₂O₃ (corundum) single crystals has been studied by means of isochronal thermal annealing of radiation-induced optical absorption (RIOA). The integral of elementary Gaussians (product of RIOA spectrum decomposition) has been considered as concentration measure of relevant oxygen-related Frenkel defects (neutral and charged interstitial-vacancy pairs, $F-H$, F^+-H). The annealing kinetics of these four ion-induced point lattice defects has been modelled in terms of diffusion-controlled bimolecular recombination reactions and compared with those earlier done for the case of corundum irradiation by fast neutrons. The changes in the parameters of interstitial (mobile component in the recombination process) annealing kinetics – activation energy E and pre-exponential factor X – in ion-irradiated crystals are considered.

Keywords: Al₂O₃; Radiation; Swift heavy ions; Radiation-induced absorption; Frenkel defects; Diffusion-controlled annealing

1. Introduction

Several metal oxides (binary ones, perovskites, spinel-structured, garnets) reveal fascinating physical-chemical properties, high melting temperature and wide optical transparency region (energy gap, E_g exceeds 7 eV) and, therefore, these single crystals and polycrystalline ceramics are widely used for different scientific and technological application. In particular, aluminum oxide (corundum, sapphire, α -Al₂O₃ with lattice structure of $R\bar{3}$ space group [1]) is exploited as a host for ruby, titanium-sapphire and color-center lasers [2–4], material for optical windows and light guides, medical and jewelry industry, substrates for electronics [5]; scintillation detectors and luminescent dosimeters of radiation [6–9] and etc. Because of high radiation tolerance, corundum is used in fission-based energetics and is considered as promising material for projected advanced and fusion reactors [10–13].

Radiation processes in α -Al₂O₃ crystals induced by incident energetic particles (neutrons, electrons, light and heavy ions) have been thoroughly investigated over many decades using different experimental methods [10,14–36]. To a large extent, the degradation of functional materials exploited under radiation environment is determined by increasing radiation damage via the creation, accumulation and aggregation of primary lattice defects, interstitial-vacancy (i-v) Frenkel pairs. In corundum, as well as in other radiation-resistant metal oxides, the formation energy of a Frenkel pair (displacement threshold energy) exceeds the E_g value by several times (see, e.g., [22] and references therein), and i-v pairs are predominantly formed due to elastic collisions of incident particles with material nuclei. It is generally accepted that such impact (displacement) mechanism is

solely responsible for the damage induced by fast fission neutrons [10,18,22,37,38]. However, some contribution of ionization losses could also be considered in case of material irradiation by swift heavy ions, which provide extremely high density of electronic excitations along ion tracks [29,31,39–42]. Irradiation with swift heavy ions causes intense local lattice disorder and efficient formation of extended defects.

Nowadays, oxygen-vacancy-related defects have been studied more completely in α -Al₂O₃ single crystals. The optical characteristics (absorption/excitation and relevant emission bands) of a single oxygen vacancy with two or one trapped electron (the classical F and F^+ center, respectively) as well as the simplest F_2 dimer centers in different charge states (from two to four electrons localized in two adjacent oxygen vacancies) have been revealed in the crystals either exposed to radiation [16,17,19,21,23,28,29,34,35] or grown under reducing atmosphere conditions (anion-deficient or thermochemically-reduced crystals [21,23,43–45]). In addition, the EPR signal of the F^+ center was revealed in neutron-irradiated corundum long ago [15], and the signal of paramagnetic dimer of two adjacent F^+ centers (total spin $S=1$) was recently detected as well [35].

The processes of thermal annealing of the radiation-induced F - and F_2 -type defects in corundum crystals have also been studied [10,19,21,25,27,32–35,43,44]. It has been established that just oxygen interstitials act as a mobile component in a temperature-stimulated recombination of complementary defects from i-v Frenkel pairs. This conclusion is based on a very high thermal stability of the F centers (up to at least 1000 °C) in thermochemically-reduced α -Al₂O₃ crystals (as well as in MgO [46]), which do not contain oxygen interstitials, while the F -center annealing in the irradiated crystals takes place at significantly lower temperatures [21,43,44].

The thermal annealing kinetics of the F -type centers in corundum crystals has been theoretically analyzed [32,47] and lately also with the involvement of two types of mobile oxygen interstitials [34,48,49]. It is notable that isolated oxygen interstitials have been revealed only recently in neutron-irradiated α -Al₂O₃ crystals [33,48]. Such single interstitial has been detected via the EPR method in a form of a superoxide ion. Until then, only the ERP signals of oxygen interstitials associated with additional imperfections (in particular, with a cation vacancy) were detected in binary metal oxides (see, e.g., [33,50]).

The present study is a logical continuation of our previous paper [36], where the accumulation of different anion Frenkel defects with fluence of 231-MeV xenon ions was studied in α -Al₂O₃ single crystals. The isochronal annealing of oxygen-related Frenkel defects (defect concentration is taken as an integral of a relevant elementary optical absorption band) has been measured in corundum crystals preliminary irradiated by energetic xenon ions with fluence varying from 5×10^{11} to 2×10^{14} cm⁻². The experimentally obtained annealing kinetics have been theoretically analyzed in terms of the diffusion-controlled reactions between two pairs of oxygen Frenkel defects.

2. Experimental

Nominally pure α -Al₂O₃ single crystals were supplied by Alineason Materials Technology GmbH. The crystal plates with dimensions of $5 \times 5 \times 0.5$ mm³ were cut off with base orientation perpendicular to the c crystal axis and polished from both sides. Using the EPR method, the concentration of Cr³⁺ impurity centers was determined as $\approx 3.2 \times 10^{15}$ cm⁻³, while commonly present Fe³⁺ ions were not detected at all (if present, significantly below 10^{14} cm⁻³).

The samples were irradiated by 231-MeV ¹³²Xe ions (flux along the c axis) with nine different fluences Φ between 5×10^{11} and 2×10^{14} cm⁻² at room temperature (RT) using the DC-60 accelerator in Astana, Kazakhstan. Based on SRIM-2013 calculations [51], the penetration depth (range) of ions into the crystals was estimated approximately as $R = 13.5$ μ m.

The optical absorption spectra were measured at RT in a wide range of 1.5–8.5 eV using two setups: a JASCO V-660 spectrometer (till 6.5 eV) and a vacuum monochromator VMR-2 with a hydrogen discharge in a flow capillary tube as a light source. In the latter case, the number of incident photons was normalized via sodium salicylate luminescence. The absorption of a pristine crystal was subtracted from the spectrum for the same sample after irradiation. This difference spectrum of the

so-called radiation-induced optical absorption (RIOA) was decomposed into Gaussians, which characterized the concentration of different point lattice defects.

The isochronal thermal annealing of the irradiated crystals was performed in an argon atmosphere as follows: a sample heating to a predetermined temperature T_{pr} ; stay at this temperature for five minutes and, finally, the removal of a quartz reactor tube with the sample out of a furnace and passive cooling down to RT. Such cycles were performed at the same conditions with the rise of T_{pr} by 20–40 K up to 1250 K. After each preheating the RIOA spectrum was measured at RT and decomposed into elementary components.

The concentration of paramagnetic centers (both impurities and radiation defects) in corundum crystals was determined by means of a tailored Bruker software and a 9.8-GHz spectrometer Bruker ELEXSYS-II E500. The estimation accuracy of paramagnetic center concentration (impurity ions or radiation defects) is about 15% (see also [36]).

3. Results and Discussion

3.1. Thermal Annealing of RIOA Bands Related to Radiation-Induced Frenkel Defects

In the present paper, we focus on the thermal annealing kinetics of oxygen-related Frenkel pairs (both charged and neutral i-v pairs) in corundum single crystals irradiated by different fluences of energetic xenon ions. According to the literature data [16,20,21,43], two optical absorption bands peaked at 4.8 and 5.3 eV are related to the F^+ center, the structure of which (V_O^\bullet in Kröger-Vink notations) is strictly confirmed by the EPR method (see, e.g., [15,35]). The absorption band, detected in thermochemically-reduced and irradiated crystals and peaked around 6.1 eV, was attributed to the F centers (a neutral defect with respect to a regular lattice, V_O^\times) [16,20,21,43].

The characteristics of oxygen interstitials, defects being complementary to vacancy-containing F and F^+ centers, have been revealed only recently. A single charged oxygen interstitial (labelled as H^- or O_i' in Kröger-Vink notations) stabilized by a trapped hole was detected in the form of superoxide ion O_2^- in a neutron-irradiated corundum by the EPR method [33,48]. The analysis of isochronal annealing of the EPR signal and RIOA spectra allowed to attribute the 5.6-eV absorption band to the H^- centers [33,34,48,49] and to suggest the connection of the ≈ 6.6 eV RIOA band with neutral oxygen interstitials (labelled as H^0 or O_i'') [34,48,49].

In the previous paper we studied the evolution of optical absorption spectra with Xe-ion fluence and confirmed/proved the radiation-induced origin of the defects responsible for the RIOA above 4 eV (F^+ , F , H^- and H^0 centers) [36]. Note that the analysis of RIOA in neutron- or ion-irradiated corundum single crystals was always performed via spectra decomposition into Gaussian components related to different types of radiation defects [33,34,36,48,49]. Figure 1 presents the examples of the RIOA spectra decomposition into Gaussians in the crystals exposed to different Xe-ion fluences (parts *a* and *c*) or after additional preheating of the irradiated crystals to prescribed temperatures T_{pr} (parts *b* and *d*). The same parameters of Gaussian components (maximum position and bandwidth) were used in [36] and the present study. The Gaussians marked by dashed lines belong to still unidentified defects and not be the subject of this article. The F_2 -type dimer centers in different charge states possess characteristic absorption bands at 2.3–4.0 eV [19,21,29,33,34,44,48], their concentration in Xe-irradiated crystals is low and these dimers are not considered in the present study.

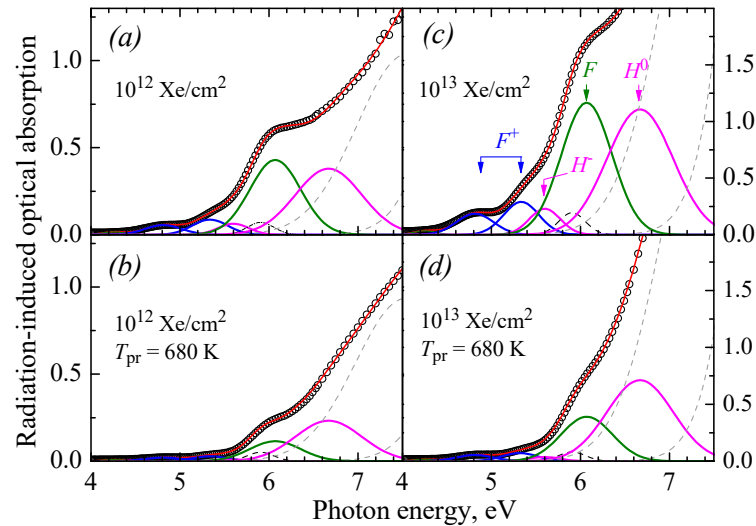


Figure 1. The RIOA spectra and their decomposition into elementary components for α - Al_2O_3 single crystals irradiated with two fluences, $\Phi = 10^{12} \text{ Xe/cm}^2$ and $\Phi = 10^{13} \text{ Xe/cm}^2$. Symbols demonstrate experimental points, the red solid line – the sum of all Gaussian components. The spectra are measured at RT after irradiation (parts a and c) and additional preheating of the irradiated crystal to $T_{\text{pr}} = 680 \text{ K}$ (parts b and d).

Figure 2 demonstrates the concentration dependences of four oxygen-related Frenkel defects on the fluence of corundum crystals irradiation with 231-MeV Xe ions (as compared to [36], irradiations with three more fluences were performed). The continuous increase of defect concentration with fluence up to $\Phi = 2 \times 10^{14} \text{ cm}^{-2}$ proves that, similar to the classic F and F^+ centers, the defects connected with the absorption Gaussians at ≈ 5.6 and $\approx 6.6 \text{ eV}$ are the irradiation-induced lattice defects.

In Figure 2, the integral of a certain Gaussian (in arbitrary units) is taken as a concentration measure of the relevant Frenkel defects. At the same time, the concentration of paramagnetic defects, in particular, the F^+ and H^- centers can directly be determined by the EPR method. Note that ion-irradiation creates defects only within a thin crystal layer and their absolute number in the crystal (amount of unpaired spins) is significantly lower than in the case of neutron irradiation. Because of the features or relevant EPR spectra, only the signal of superoxide ions O_2^- (an H^- stabilized by a trapped hole) was clearly registered in our samples. At $\Phi = 10^{13} \text{ Xe cm}^{-2}$, the concentration of H^- interstitials was estimated as $N = 1.5 \times 10^{18} \text{ cm}^{-3}$, the value approximately doubles for $\Phi = 10^{14} \text{ cm}^{-2}$ ($N = 3.2 \times 10^{18} \text{ cm}^{-3}$), and the concentration of O_2^- reaches $N = 3.55 \times 10^{18} \text{ cm}^{-3}$ in the case of the highest $\Phi = 2 \times 10^{14} \text{ cm}^{-2}$. The accuracy of concentration estimation is about 15% (for details see [36]). Note that in a neutron-irradiated corundum the EPR signals of both the F^+ and O_2^- centers were clearly detectable and the concentration of these paramagnetic defects was practically equal [33,48].

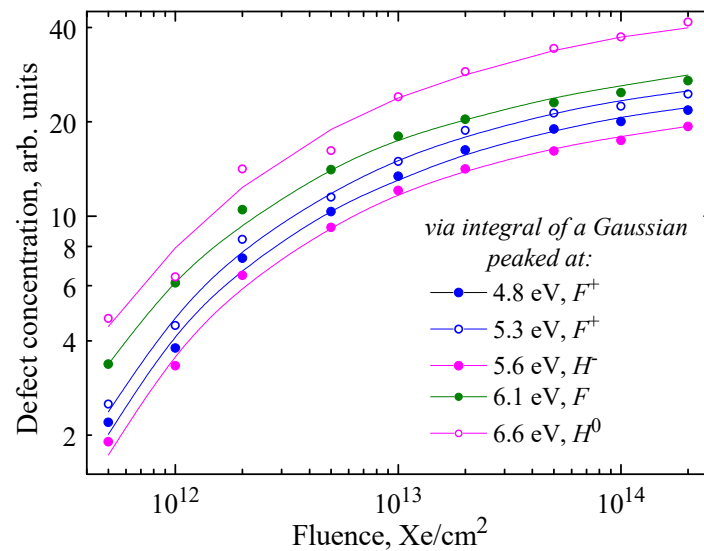


Figure 2. Dependences of the defect concentration on the Xe-ion fluence in α -Al₂O₃ single crystals. Integral of a relevant Gaussian is used as a measure of different Frenkel defects. Solid lines serve as guides for the eye.

Based on the above-described decomposition procedure, the thermal annealing of four Frenkel defects has been studied in α -Al₂O₃ single crystals preliminary irradiated with different fluences of energetic xenon ions. The decomposition of RIOA spectra measured at RT after each preheating to a predetermined temperature T_{pr} (see examples in Figure 1b,d) allowed to construct concentration dependences on preheating temperatures for different defects (via integral of a relevant Gaussian) induced by different ion fluences.

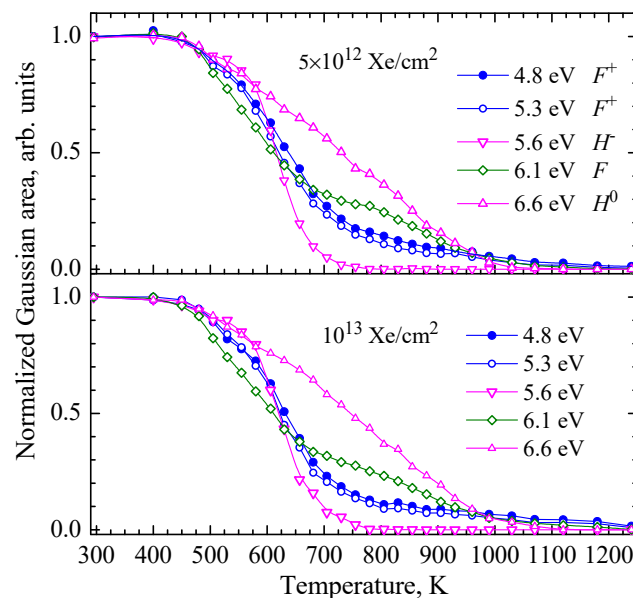


Figure 3. Normalized thermal annealing curves of RIOA Gaussians (maxima at indicated photon energy) connected with oxygen-related Frenkel defects for corundum crystals irradiated by 231-MeV Xe ions with different fluences. Integral of an elementary Gaussian serves as a measure of relevant defect concentration. Solid lines serve as guides for the eye.

Figure 3 presents the examples of such isochronal annealing kinetics, which describe the thermal stability of a certain defect type, constructed for the corundum crystals ion-irradiated with $\Phi = 5 \times 10^{12} \text{ cm}^{-2}$ and $\Phi = 10^{13} \text{ cm}^{-2}$. The normalization of annealing curves simplifies the separation of temperature-stability regions typical of different defects. It is clearly seen that only the annealing of

charged interstitials H^- could be roughly considered as one-stage process, while the decay of other Frenkel defects takes place in several stages. The stability of the F^+ centers has been estimated via two RIOA Gaussians peaked around 4.8 and 5.3 eV, the annealing kinetics of which practically coincide (deviations in the region with rather low values of optical density illustrate the experimental accuracy).

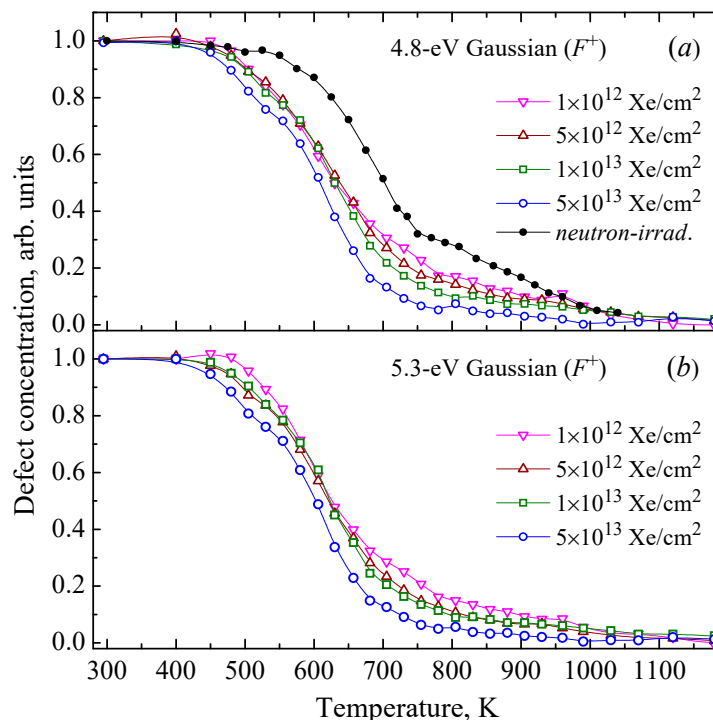


Figure 4. Normalized annealing curves for the F^+ centers induced by 231-MeV Xe ions or fast neutrons in α - Al_2O_3 single crystals. Integral of a RIOA Gaussian at $I_{\text{max}}=4.81$ eV (a) and $I_{\text{max}}=5.33$ eV (b) serves as a measure of defect concentration. Solid lines serve as guides for the eye.

Of particular interest is the influence of irradiation fluence that should lead to different space topologies of radiation-induced defects on the kinetics of recombination processes between complementary Frenkel defect. The experimentally obtained annealing curves of the F , F^+ , H^- and H^0 defects induced by four different Xe-irradiation fluences are presented in Figures 4 to 6. In comparison, the experimental annealing curves for the same Frenkel defects constructed on the basis of the relevant RIOA Gaussians in neutron-irradiated corundum (see our previous publications [33,34,48]) are shown in Figures 4-6 as well.

It is notable that in neutron-irradiated corundum crystals intense EPR signals related to the F^+ and H^- (O_2^-) defects allowed precise registration of the defect concentration dependence on preheating temperature. It was clearly demonstrated that such dependences for paramagnetic F^+ and H^- centers practically coincide with those constructed on the basis of relevant RIOA Gaussians [33,34,48]. Unfortunately, the EPR method was not applicable for thermal annealing in case of Xe-irradiation. Due to the small range of energetic Xe ions (around 13.5 μm), the absolute number of ion-induced defects was too low, up to two orders of magnitude lower with respect to the crystals homogeneously colored in a whole volume by fast neutrons. As a result, in the present study, the annealing of Frenkel defects was studied only via the defect-related RIOA Gaussians (band integral proportional to defect concentration).

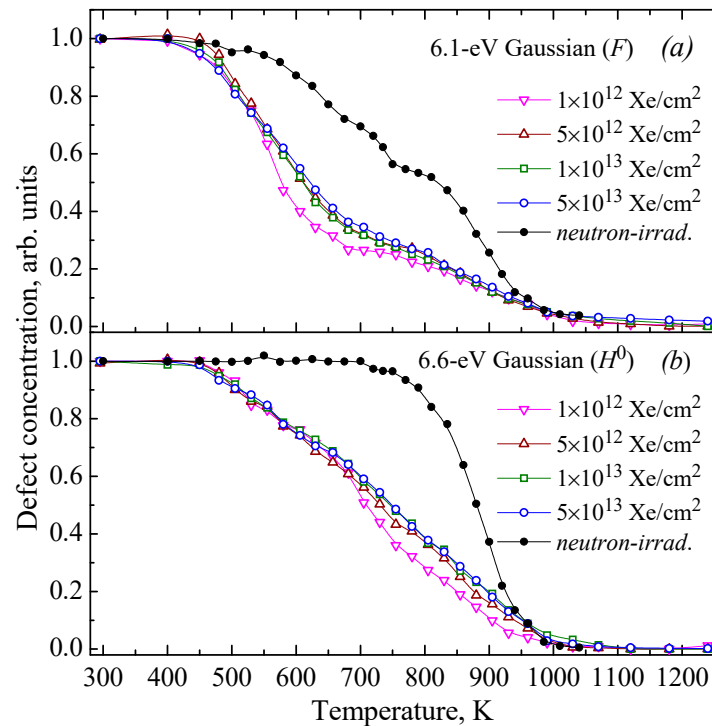


Figure 5. Normalized annealing curves for the F and H^0 centers induced by 231-MeV Xe ions or fast neutrons in α -Al₂O₃ single crystals. Integral of a RIOA Gaussian at $I_{\max}=6.07$ eV (a) and $I_{\max}=6.67$ eV (b) serves as a measure of a relevant defect concentration. Solid lines serve as guides for the eye.

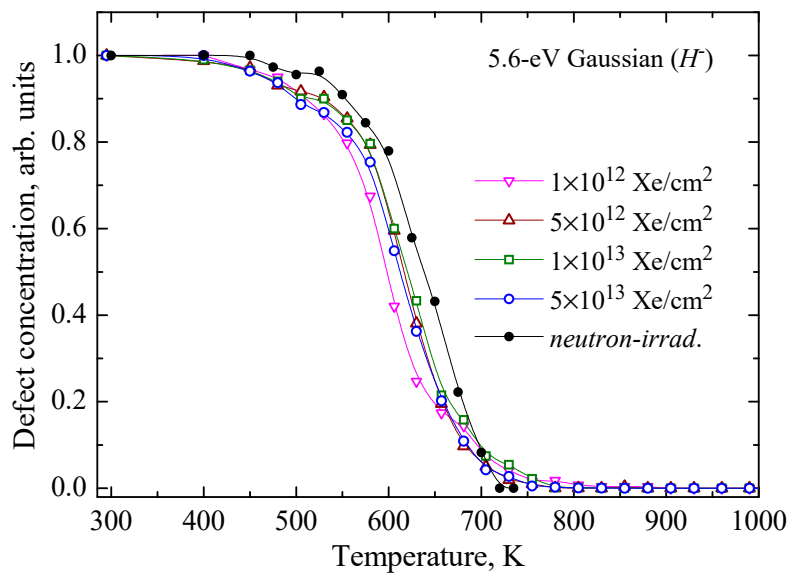


Figure 6. Normalized annealing curves for the H^- centers induced by 231-MeV Xe ions or fast neutrons in α -Al₂O₃ single crystals. Integral of a RIOA Gaussian ($I_{\max}=5.6$ eV) serves as a measure of defect concentration. Solid lines serve as guides for the eye.

It is clearly seen that only the annealing kinetics of the H^- centers (RIOA at 5.6 eV) is very similar for the both cases of irradiation (see Fig. 6), while, in general, the annealing of other Frenkel defects in ion-irradiated crystals starts at lower temperatures than in neutron-irradiated crystals (see Figures 4 and 5). Note that the thermal annealing kinetics of neutron-induced Frenkel defect pairs (F^+-H^- and $F-H^0$) have already been modelled in terms of diffusion-controlled biomolecular reactions and the involvement of differently changed mobile oxygen interstitials [34,48,49]. The present study is a

logical continuation of such theoretical analysis for the case of oxygen-related defect creation by energetic ions with different fluences.

3.2. Method and Kinetics Modelling

In this Section, we discuss the main theoretical results by comparing two sets of defect annealing kinetics in the same material ($\alpha\text{-Al}_2\text{O}_3$), subjected to different types of irradiation: neutrons and swift heavy ions. The case of neutron irradiation has been thoroughly investigated in our previous studies [34,48,49], where we developed a model describing the underlying processes and introduced an appropriate mathematical framework for defect recombination kinetics. The details of this model and the associated solution methods are extensively covered in the cited references; therefore, only key definitions and concepts will be summarized here.

We treat the neutron irradiation case as a reference or benchmark and seek to understand why the kinetics change qualitatively – sometimes appearing anomalous – under energetic ion irradiation. The model introduced in our studies [34,48,49] is based on the assumption that irradiation generates both neutral and charged Frenkel defects, while maintaining overall electrical neutrality. Specifically, two types of anion Frenkel defect pairs are created: charged defect pairs (F^+H^-) and neutral defect pairs ($F-H^0$).

Initially, the concentrations of each electron-type vacancy-containing centers and their complementary interstitials – either neutral (H^0) or charged (H^-) – are equal. These concentrations evolve through recombination processes, which, in turn, affect the relative proportions of neutral and charged radiation defects. Both neutral and charged interstitials can recombine not only with their respective counterparts but also with other types of vacancy-containing centers. The recombination rates vary, depending on the defect charges, with Coulomb attraction accelerating recombination between oppositely charged defects (see, e.g., [49]).

The annealing process in this model is formally a complex one due to the interaction of four defect species. However, the analysis is simplified by the fact that all recombination events are bimolecular and diffusion-controlled. The fundamental expression governing these processes is the Smoluchowski relation for the reaction rate [49,52]: $K = 4\pi DR$, where D is the relative diffusion coefficient of the reacting species, and R is the recombination radius.

In oxide materials like $\alpha\text{-Al}_2\text{O}_3$, it is well-established that vacancies exhibit significantly lower mobility than interstitials in the temperature range relevant to annealing. As a result, the mobility of vacancies can be neglected, $D_F \approx 0$ and $D_{F^+} \approx 0$, and only the interstitials (H^0 and H^-) are mobile and govern the kinetics. These interstitials migrate via thermally activated jumps characterized by activation energies E_a and E_b , leading to diffusion coefficients of the form:

$$D_{H^-} = D_a \exp\left(-\frac{E_a}{k_B T}\right), \quad (1)$$

$$D_{H^0} = D_b \exp\left(-\frac{E_b}{k_B T}\right), \quad (2)$$

where D_a and D_b are the respective pre-exponential factors.

When solving the system of kinetic equations describing bimolecular recombination among the four defect types [49], the diffusion pre-factors appear as a part of effective process pre-exponentials:

$$X_a = D_a N_0 R / \beta, \quad (3)$$

$$X_b = D_b N_0 R / \beta. \quad (4)$$

These expressions combine several physical and experimental parameters, including the diffusion coefficients (D_a and D_b), recombination radius R , total concentration of vacancy-containing centers N_0 (equal to that of interstitials), and the effective heating rate β . Here, β is defined as a constant rate of temperature increase during annealing, $\beta = \frac{T_{\max} - T_{\min}}{\Delta t} = \text{const.}$ Overall, this kinetic

analysis provides a pathway to infer the mobility of interstitial atoms – information that is otherwise challenging to obtain directly

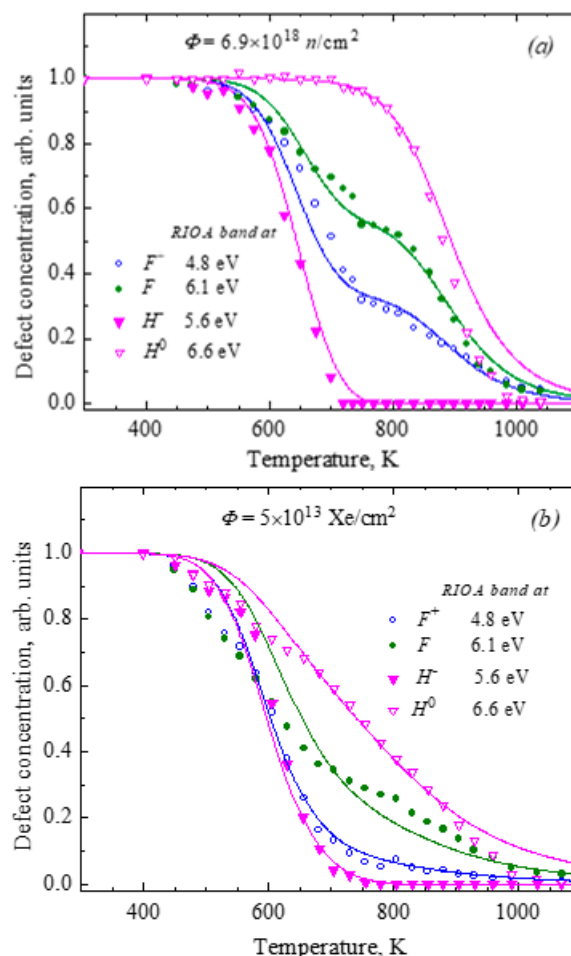


Figure 7. The normalized experimental annealing kinetics for four types of radiation-induced Frenkel defects (symbols – on the basis of relevant RIOA Gaussians) and their theoretical analysis (full lines) for α - Al_2O_3 single crystals exposed to fast fission neutrons (part *a*, see also [48,49]) and 231-MeV xenon ions (part *b*).

Figure 7 presents a comparison of the annealing kinetics for four types of Frenkel defects, whose recombination involves a complex interplay of cross-reactions, under two irradiation conditions: fast neutron irradiation (part *a*) and swift heavy ion irradiation (*b*). Since the annealing kinetics is largely governed by mobile interstitials, particular attention should be paid to the RIOA bands corresponding to two differently charged interstitials: the band peaked at 5.6 eV is related to the H^- centers, while the maximum of the tentative H^0 center absorption is around 6.6 eV.

For both irradiation types, the experimental kinetics of the H^- centers appears to be robust. This reliability stems from the fact that in the relevant energy range, spectral decomposition into Gaussian components is straightforward. As a result, experimental data points align smoothly with theoretical curves, and associated errors are minimal. Consequently, the agreement between theory and experiment for the H^- centers in Figure 7 can be considered as very good.

In contrast, the two kinetics of neutral H^0 centers present significant challenges. At higher energies (above a certain threshold), experimental measurements of RIOA are not feasible. In the case of ion-irradiation, the influence (overlapping) of the Gaussians of unknown origin peaked above 7 eV (labelled by dashed lines in Figure 1) on the bands of the H^0 and even F centers is significant. In a neutron-irradiated corundum, the isolated maximum of the F -absorption is clearly registered at 6.07 eV, and this RIOA band intensity decreases till 7 eV by more than two times [33,34,48,49]. On the other hand, there is no isolated F -band in the RIOA spectra of Xe-irradiated crystals (see Fig. 1, parts

a and *c*); a relative contribution of high-energy Gaussians (tentatively connected with more complex structural defects) increases with T_{pr} (see Figure 1, parts *b* and *d*). According to Figure 8, these intense Gaussianse are cleary detectable even after $T_{\text{pr}} = 1240$ K, i.e. total annealing of the Frenkel defects under consideration.

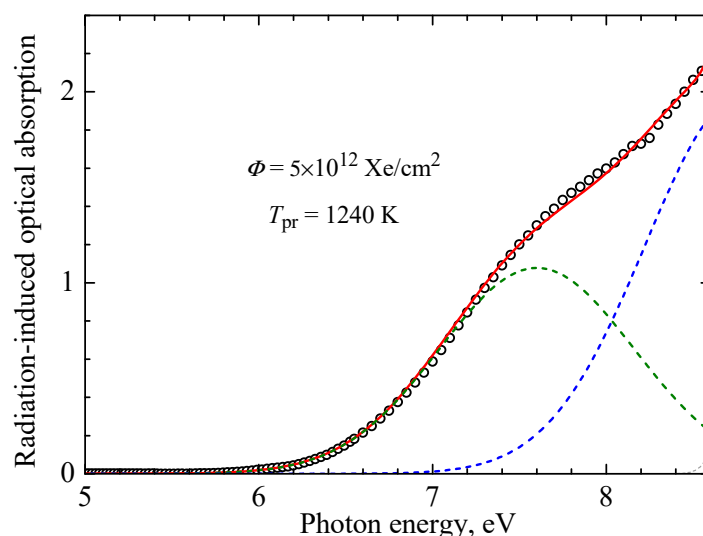


Figure 8. The RIOA spectrum and its decomposition into elementary components for $\alpha\text{-Al}_2\text{O}_3$ single crystals irradiated with $\Phi = 5 \times 10^{12} \text{ Xe/cm}^2$ and additionally preheated to $T_{\text{pr}} = 1240$ K. Symbols demonstrate experimental points, the red solid line – the sum of Gaussian components. The spectrum was measured at RT.

As it is seen in Figure 7, the theoretical and experimental curves for the H^0 centers diverge at high temperatures. Specifically, the amplitudes of bands reconstructed from these problematic spectral regions decay too rapidly, in contradiction with the expected behavior dictated by chemical kinetics. Despite these difficulties, the diffusion-controlled model used in this study demonstrates high stability. In Figure 7, we compared experimental results with theoretical predictions based on the RIOA band, peaked at 4.8 eV and ascribed to the F^+ center. Note that almost the same arrangement of modelled curves has been obtained taking the 5.3 eV RIOA band as a measure of the F^+ centers (both bands are related to the same defect).

Our less obvious finding is concerned with the role of radiation fluence. Previous studies (see, e.g., [32,47]) have shown that fluence can significantly impact the annealing kinetics under electron, proton, and neutron irradiation, particularly altering diffusion activation energies. However, for heavy ion irradiation, our analysis indicates that annealing kinetics are largely fluence-independent. This is consistent with the level of agreement observed in Figure 7b. Notably, the reducing fluence increases experimental uncertainty and limits the scope for theoretical analysis. Consequently, it was impossible to reach the fluence regime when neutron and ion irradiation data might hypothetically converge. So far, the results suggest that switching to ion irradiation qualitatively alters the annealing behavior. This weak or even negligible kinetics dependence on fluence during ion irradiation has also been previously observed [53], though a definitive explanation remains elusive.

As a result of fitting the theory to the experimental kinetics using the least squares method, we obtain the characteristics of the interstitials, which are summarized in Table 1. Before discussing the obtained numerical values, a necessary comment should be done. It is easy to see that in the case of neutron irradiation, both kinetics for interstitials show a step, sharply falling in the temperature range of 100-200 K from the maximum to the minimum values. Meanwhile, to determine the activation energy with high accuracy, it is desirable to analyze the kinetic curves in a wide temperature range. Here, there is an analogue of the uncertainty relation between the temperature range and the error in determining the energy. This uncertainty was eliminated in Refs. [34,48,49] by equating the values of the diffusion activation energies to independent theoretical estimates, $E_a = 0.80$ eV and $E_b = 1.20$ eV, found for corundum by quantum chemistry methods (see [48,49] and references therein). The

accuracy of these values can be estimated as 20 %. The reason is trivial: the minimum of the optimized function is poorly expressed due to the noted uncertainty relation between energy and temperature.

As a result, for the case of neutron irradiation, it can be concluded that the inequality $E_a < E_b$ is a reliably established fact (charged interstitials are more mobile than neutral ones), but the values of the activation energies in Table 1 are only rough estimates. Therefore, for charged interstitials, other results are also quite acceptable.

Table 1. The obtained migration energies of interstitials E and corresponding pre-exponential factors X

Irradiation source	Fluence	E_a (eV)	X_a (K ⁻¹)	E_b (eV)	X_b (K ⁻¹)
neutrons, Ref. [49]	$6.9 \times 10^{18} \text{ cm}^{-2}$	0.80	2×10^3	1.20	2×10^4
Xe-ions	$5.0 \times 10^{13} \text{ cm}^{-2}$	0.65	3×10^2	0.50	6×10^0

A comparison of the parts (a) and (b) in Figure 7 demonstrates that the transition from neutron-to ion-irradiation qualitatively changes the kinetics of radiation defect annealing: the characteristic step of annealing of the H^0 interstitials disappears and, instead, an unusual form of defect concentration decline, along a straight line with a certain slope, takes place in a large temperature range (about 500 K). Nevertheless, Table 1 shows that the experimental kinetics can be approximated by theoretical ones within the framework of the same model involving four defect types, although the parameter values are different. It remains to clarify which parameter changes are responsible for the noted visual changes.

For ion irradiation, the migration energy of charged interstitials $E_a=0.65$ eV, was obtained by fitting to the experiment via the least square method, without using estimates found by other methods. It can be seen that the found value falls within the uncertainty interval (20 %) that we discussed in the case of neutron irradiation. There is every reason to admit that the H interstitials have the same nature for both irradiation types. Moreover, a comparison of the corresponding values of the kinetic pre-factors: $X_a=2 \times 10^3 \text{ K}^{-1}$ for fast neutrons and $X_a=3 \times 10^2 \text{ K}^{-1}$ for energetic Xe ions, show a small difference. Let us pay also attention to the eq. (3): when changing the radiation source from neutrons to ions, there is no guarantee that the same values of the initial concentration of the vacancy-containing centers (F and F^+) are preserved. Therefore, a small discrepancy between the numerical values of the parameters is quite explainable.

For neutral interstitials H^0 , the data in Table 1 reveal not only a substantial reduction in the activation energy from $E_b=1.20$ eV to $E_b=0.50$ eV, but also a dramatic change in the pre-exponential factor, by several orders of magnitude. Given the rough nature of these estimates, we cannot definitively claim that the previously assumed inequality $E_a < E_b$ has been reversed under ion irradiation. However, it is evident that the activation energies for the two types of interstitials have become comparable, which is a highly unusual conclusion.

It is important that within this scenario, the four-orders-of-magnitude drop in the X_b prefactor can no longer be attributed solely to the changes in the F -type center concentration. This kind of simultaneous decrease in both the activation energy and pre-exponential factor has been analyzed in detail in Ref. [47], and is considered as a manifestation of a well-known phenomenon in disordered systems physics – the Meyer-Neldel rule [54,55]. According to this rule, a diminishing in activation energy E due to increasing material disorder is compensated by a corresponding drop in the diffusion prefactor X .

A plausible interpretation of the presented findings is that irradiation induces structural disordering, possibly progressing from a nearly perfect crystalline state toward an almost amorphous structure [47]. Under heavy ion irradiation, such disordering is likely to be especially pronounced – detailed mechanisms may include the formation of collision cascades, defect clusters, extended defects, local lattice disordering (see, e.g., [22,31,41,42]). Our analysis suggests that the key difference in the annealing kinetics between neutron and ion irradiation arises from the higherr degree of local

lattice disordering introduced by ions. This disorder primarily affects neutral interstitials, significantly altering their kinetic behavior.

Of particular interest are the features of two kinetics for the F and F^+ centers. In Figure 7a, the stepwise structure of these kinetics with a very unusual behavior is clearly visible: the decay begins at approximately the same temperature, and the curves initially diverge (fork), but then converge again at higher temperatures. As it is shown in detail in [34,49], such behavior is due to the Coulomb interaction of charged defects. As a result, the annealing curve of charged F^+ centers always pass *below* the analogous curve for the neutral centers. In Figure 7b, the stepwise structure of the kinetics and the anomalous behavior (divergence or convergence of the curves) are expressed significantly weaker. Such discrepancy between the kinetics for neutron- and ion-irradiation has a simple reason. So far in the discussion, we did not pay attention to a trivial fact: radiation creates pairs of charged and neutral defects, but in different proportions. A parameter w^+ was introduced in Refs. [34,48,49] as the fraction of charged defects when the annealing begins. The kinetics shown in Figure 7 (parts a and b) correspond to different values of this parameter, namely, $w^+ = 0.55$ for neutron irradiation and $w^+ = 0.75$ for ion irradiation. In other words, in the case (a), the initial concentration of charged and neutral defects practically coincides, but in the case (b), these same concentrations are related as three to one. Meanwhile, the study [49] shows that such asymmetry in the initial concentrations leads to a systematic shift in the kinetics of the F and F^+ centers, bringing them close to the annealing curve for the H -charged interstitials. Just such shift effect can be seen in Figure 7b.

4. Conclusions

The thermal stability of oxygen-related Frenkel defects created in α - Al_2O_3 single crystals at room temperature by 231-MeV ^{132}Xe (fluence from 5×10^{11} to $2 \times 10^{14} \text{ cm}^{-2}$) has been evaluated. Taking the integral of elementary absorption band (obtained via decomposition of RIOA spectra into Gaussians) as a measure of the relevant defect concentration, the dependences of defect concentration on preheating temperature (isochronal annealing regime up to 1250 K) have been constructed.

Such annealing curves for the classical vacancy-containing F and F^+ centers (RIOA bands peaked at 6.1 eV and 4.8 eV, respectively) as well as complementary Frenkel defects – charged and neutral oxygen interstitials – H and H centers (bands at 5.6 eV and ≈ 6.6 eV) – have been theoretically analyzed in terms of diffusion-controlled bimolecular recombination reactions. In addition, annealing kinetics of the F^+-H^- and $F-H^0$ Frenkel pairs in Xe-irradiated crystals have been compared with those studied earlier in fast-neutron-irradiated corundum (see our previous studies [34,48,49]).

A comparison of the diffusion parameters extracted for neutron and Xe irradiation reveals that the migration energies for both charged and neutral interstitials are reduced in the latter case, very likely due to stronger structural disordering upon irradiation (according to the Meyer-Neldel rule discussed above).

Author contributions: Conceptualization E.A.K., A.L.; Formal analysis V.N.K., V.S., I.K., E.S.; Investigation G.B., I.K., A.P., V.S.; Methodology E.A.K., V.N.K., A.L.; E.S. V.S.; Resources R.A., G.B., Visualization R.A., A.P.; Writing-original draft – A.L., V.N.K.; Writing-review&editing E.A.K., V.S., E.S. All authors have read and agreed to the published version of the manuscript.

Funding: The study has been carried out within the framework of the EUROfusion Consortium, funded by the European Union via the Euratom Research and Training Programme (Grant Agreement No 101052200 – EUROfusion). Views and opinions expressed are however those of the author(s) only and do not necessarily reflect those of the European Union or the European Commission. Neither the European Union nor the European Commission can be held responsible for them. This work was partially supported by the Estonian Research Council grant (PRG 2031), the Latvian Council for Science (LZP grant LZP-2024/1-0159) and the Committee of Science of the Ministry of Science and Higher Education of the Republic of Kazakhstan (Grant No. AP19574768).

Data availability Statement: The processed data are available on demand from the corresponding author.

Conflict of Interests: The authors declare no conflict of interests.

References

1. W.E. Lee, K.P.D. Lagerlof, Structural and electron diffraction data for sapphire (α -Al₂O₃), J. Electron Microsc. Tech. 2 (1985) 247-258.
2. T.H. Maiman, Stimulated Optical Radiation in Ruby, Nature 187 (1960) 493-494.
3. P.F. Moulton, Spectroscopic and laser characteristics of Ti:Al₂O₃, Opt. Soc. Am. B 3 (1986) 125-133.
4. T.T. Basiev, S.B. Mirov, V.V. Osiko, Room-temperature color center lasers, IEEE J. Quantum Electron. 24 (1988) 1052-1069.
5. E.R. Dobrovinskaya, L.A. Lytvynov, V. Pishchik, Application of Sapphire (Chapter 1, pp. 1-54), in: Sapphire, Springer: Boston, MA 2009.
6. S.M. Luca, N. Coron, C. Dujardin, H. Kraus, V.B. Mikhailik, M.-A. Verdier, P.C.F. Di Stefano, Scintillating and optical spectroscopy of Al₂O₃:Ti for dark matter searches, Nucl. Instrum. Meth. A 606 (2009) 545-551.
7. M.S. Akselrod, V.S. Kortov, D.J. Kravetsky, V.I. Gotlib, Highly sensitive thermoluminescent anion-defective α -Al₂O₃:C single crystal detectors, Radiat. Prot. Dosim. 32 (1990) 15-20.
8. S.W.S. McKeever, M.S. Akselrod, L.E. Colyott, N. Agersnap Larsen, J.C. Polf, V.H. Whitley, Characterisation of Al₂O₃ for use in thermally and optically stimulated luminescence dosimetry. Radiat. Prot. Dosim. 84 (1999) 163-168.
9. V.S. Kortov, S.V. Zvonarev, A.N. Kiryakov, D.V. Ananchenko, Dosimetric phosphor based on oxygen-deficient alumina ceramics, Radiat. Meas. 90 (2016) 196-200.
10. G.P. Pells, Radiation damage effects in alumina, J. Am. Ceram. Soc. 77 (1994) 368-377.
11. S.M. Gonzales de Vicente, E.R. Hodgson, T. Shikama, Functional materials for tokamak in-vessel systems – status and applications, Nucl. Fusion 57 (2017) 092009.
12. D.A. Blokhin, V.M. Chernov, I. Blokhin, Nuclear and physical properties of dielectrics under neutron irradiation in fast (BN-600) and fusion (DEMO-S) reactors, Phys. Atom. Nuclei 80 (2017) 1279-1284.
13. G.S. Was, D. Petti, S. Ukai, S. Zinkle, Materials for future nuclear energy systems, J. Nucl. Mater. 527 (2019) 151837.
14. F.T. Gamble, R.H. Bartram, C.G. Young, O.R. Gilliam, P.W. Levy, Electron-spin resonances in reactor-irradiated aluminium oxide, Phys. Rev. 138 (1965) A577-A583.
15. S.Y. La, R.H. Bartram, R.T. Cox, The F⁺ center in reactor-irradiated aluminum oxide, J. Phys. Chem. Solids 34 (1973) 1079-1086.
16. K.H. Lee, J.H. Crawford, Electron centers in single-crystal Al₂O₃. Phys. Rev. B 15 (1977) 4065-4070.
17. B.D. Evans, M. Stapelbroek, Optical properties of the F⁺ center in crystalline Al₂O₃, Phys. Rev. B 18 (1978) 7089-7098.
18. J.H. Crawford, A review of neutron radiation damage on corundum crystals, J. Nucl. Mater. 108-109 (1982) 644-654.
19. K. Atobe, N. Nishimoto, M. Nakagawa, Irradiation-induced aggregate centers in single crystal Al₂O₃, Phys. Stat. Solidi A 89 (1985) 155-162.
20. Y. Chen, M.M. Abraham, D.F. Pedraza, Radiation damage in Al₂O₃ crystals implanted with 3.8 MeV Fe²⁺ ions, Nucl. Instrum. Meth. B 59-60 (1991) 1163-1166.
21. B.D. Evans, A review of the optical properties of anion lattice vacancies, and electrical conduction in α -Al₂O₃: their relation to radiation-induced electrical degradation, J. Nucl. Mater. 219 (1995) 202-223.
22. S.J. Zinkle, C. Kinoshita, Defect production in ceramics. J. Nucl. Mater. 251 (1997) 200-217.
23. A.I. Surdo, V.S. Kortov, V.A. Pustovarov, Luminescence of F and F⁺ centers in corundum upon excitation in the interval from 4 to 40 eV, Rad. Meas. 33 (2001) 587-591.
24. V.A. Skuratov, K.J. Gun, J. Stano, D.L. Zagorski, In situ luminescence as monitor of radiation damage under swift heavy ion radiation, Nucl. Instrum. Meth. B 245 (2006) 194-200.

25. M. Izerrouken, T. Benyahia, Absorption and photoluminescence study of Al_2O_3 single crystal irradiated with fast neutrons, Nucl. Instrum. Meth. B 468 (2010) 2987-2990.
26. C.M. Petrie, W. Windl, T.E. Blue, In-situ reactor radiation-induced attenuation in sapphire optical fibers, J. Am. Ceram. Soc. 97 (2014) 3883-3889.
27. M. Izerrouken, Y. Djouadi, H. Zirour, Annealing process of F-and F^+ -centers in Al_2O_3 single crystal induced by fast neutrons irradiation, Nucl. Instrum. Meth. B 319 (2014) 29-33.
28. M. Malo, A. Morono, E.R. Hodgson, In situ luminescence qualification of radiation damage in aluminas: F-aggregation and Al colloids, Fusion. Eng. Des. 89 (2014) 2179-2183.
29. M.L. Crespillo, J.T. Graham, Y. Zhang, W.J. Weber, In-situ luminescence monitoring of ion-induced damage evolution in SiO_2 and Al_2O_3 , J. Lumin. 172 (2016) 208-2018.
30. J.M. Costantini, Y. Watanabe, K. Yasuda, M. Fasoli, Cathodo-luminescence of color centers induced in sapphire and yttria-stabilized zirconia by high-energy electrons, J. Appl. Phys. 121 (2017) 153101
31. C. Grygiel, F. Moisy, M. Sall, H. Lebius, E. Balanzat, T. Madi, T. Been, D. Marie, I. Monnet, In-situ kinetics of modifications induced by swift heavy ions in Al_2O_3 : Colour centre formation, structural modification and amorphization, Acta Mater. 140 (2017) 157-167
32. A.I. Popov, A. Lushchik, E. Shablonin, E. Vasil'chenko, E.A. Kotomin, A.M. Moskina, V.N. Kuzovkov, Comparison of the F-type center thermal annealing in heavy-ion and neutron irradiated Al_2O_3 single crystals, Nucl. Instrum. Meth. B 433 (2018) 93-97.
33. V. Seeman, A. Lushchik, E. Shablonin, G. Frieditis, D. Gryaznov, A. Platonenko, E.A. Kotomin, A.I. Popov, Atomic, electronic and magnetic structure of an oxygen interstitial in neutron-irradiated Al_2O_3 single crystals, Sci. Reports 10 (2020) 15852
34. A. Lushchik, V.N. Kuzovkov, A.I. Popov, G. Frieditis, V. Seeman, E. Shablonin, E. Vasil'chenko, E.A. Kotomin, Evidence for the formation of two types of oxygen interstitials in neutron-irradiated α - Al_2O_3 single crystals, Sci. Reports 11 (2021) 20909.
35. V. Seeman, A.I. Popov, E. Shablonin, E. Vasil'chenko, A. Lushchik, EPR-active dimer centers with $S = 1$ in α - Al_2O_3 single crystals irradiated by fast neutrons, J. Nucl. Mater. 569 (2022) 153933.
36. G. Baubekova, R. Assylbayev, E. Feldbach, A. Krasnikov, I. Kudryavtseva, A. Podelinska, V. Seeman, E. Shablonin, E. Vasil'chenko, A. Lushchik, Accumulation of oxygen interstitial-vacancy pairs under irradiation of corundum single crystals with energetic xenon ions, Rad. Meas. 179 (2024) 107324.
37. F.W. Clinard, Jr., L.W. Hobbs, in: Physics of Radiation Effects in Crystals, ed. R.A. Johnson and A.N. Orlov (Elsevier, Amsterdam, 1986) Chapter 7.
38. K. Nordlund, S.J. Zinkle, A.E. Sand, F. Granberg, R.S. Averbach, R.E. Stoller, T. Suzudo, L. Malerba, F. Banhart, W.J. Weber, F. Willaime, S.L. Dudarev, D. Simeone, Primary radiation damage: A review of current understanding and models. J. Nucl. Mater. 512 (2018). 450-479.
39. N. Itoh, D.M. Duffy, S. Khakshouri, A.M. Stoneham, Making tracks: electronic excitation roles in forming swift heavy ion tracks, J. Phys.: Condens. Matter 21 (2009) 474205.
40. A. Lushchik, T. Kärner, Ch. Lushchik, K. Schwartz, F. Savikhin, E. Shablonin, A. Shugai, E. Vasil'chenko, Electronic excitations and defect creation in wide-gap MgO and $\text{Lu}_3\text{Al}_5\text{O}_{12}$ crystals irradiated with swift heavy ions, Nucl. Instrum. Meth. B 286 (2012) 200-208.
41. W. Wesch, E. Wendler (Eds), E. *Ion beam modification of solids*, (Springer Series in Surface Sciences, vol. 61) Springer Nature, 2016.
42. M.L. Crespillo, F. Agulló-López, A. Zucchiatti, Cumulative approaches to track formation under swift heavy ion (SHI) irradiation: Phenomenological correlation with formation energies of Frenkel pairs. Nucl. Instrum. Meth. B 394 (2017) 20-27.
43. K.H. Lee, J.H. Crawford, Additive coloration of sapphire. Appl. Phys. Lett. 33 (1978) 273-275.
44. R. Ramírez, M. Tardío, R. Gonzalez, J.E. Munoz Santiuste, M.R. Kokta, Optical properties of vacancies in thermochemically reduced Mg-doped sapphire single crystals, J. Appl. Phys. 101 (2007) 123520.
45. Yu. Zorenko, K. Fabisiak, T. Zorenko, A. Mandowski, Qi Xia, M. Batentschuk, J. Friedrich, G. Zhusupkalieva, Comparative study of the luminescence of $\text{Al}_2\text{O}_3\text{:C}$ and Al_2O_3 crystals under synchrotron radiation excitation, J. Lumin. 144 (2013) 41-44.
46. Y. Chen, J.L. Kolopus, W.A Sibley, Luminescence of the F^+ center in MgO , Phys. Rev. 186 (1969) 865-870.

47. E. Kotomin, V. Kuzovkov, A.I. Popov, J. Maier, R. Vila, Anomalous kinetics of diffusion-controlled defect annealing in irradiated ionic solids. *J. Phys. Chem. A* 122 (2018) 28-32.
48. A. Lushchik, V. Seeman, E. Shablonin, E. Vasil'chenko, V.N. Kuzovkov, E.A. Kotomin, A.I. Popov, Detection of hidden oxygen interstitials in neutron-irradiated corundum crystals, *Opt. Mater.: X*, 14 (2022) 100151
49. A. Lushchik, V.N. Kuzovkov, I. Kudryavtseva, A.I. Popov, V. Seeman, E. Shablonin, E. Vasil'chenko, E.A. Kotomin, The two types of oxygen interstitials in neutron-irradiated corundum single crystals: Joint experimental and theoretical study, *Phys. Stat. Solidi B* 259 (2022) 2100317.
50. L.E. Halliburton, L.A. Kappers, Radiation-induced oxygen interstitials in MgO. *Solid State Commun.* 26 (1978) 111-114.
51. J.F. Ziegler, M.D. Ziegler, J.P. Biersack, SRIM - The stopping and range of ions in matter (2010), *Nucl. Instrum. Meth. B* 268 (2010) 1818-1823.
52. M.V. Smoluchowski, Versuch Einer Mathematischen Theorie der Koagulationskinetik kolloider Losungen, *Z. Phys. Chem. B* 92 (1917) 129-168.
53. V.N. Kuzovkov, E.A. Kotomin, A. Lushchik, A.I. Popov, E. Shablonin, The annealing kinetics of the *F*-type defects in MgAl₂O₄ spinel single crystals irradiated by swift heavy ions, *Opt. Mater.* 147 (2024) 11473.3
54. W. Meyer, H. Neldel, Concerning the relationship between the energy constant epsilon and the quantum constant alpha in the conduction-temperature formula in oxydising semi conductors. *Physikalische Zeitschrift* 38 (1937), 1014-1019.
55. A.G. Jones, Compensation of the Meyer-Neldel Compensation Law for H diffusion in minerals. *Geochem., Geophys., Geosyst.* 15 (2014) 2616-2631.

Disclaimer/Publisher's Note: The statements, opinions and data contained in all publications are solely those of the individual author(s) and contributor(s) and not of MDPI and/or the editor(s). MDPI and/or the editor(s) disclaim responsibility for any injury to people or property resulting from any ideas, methods, instructions or products referred to in the content.